A&A 372, 768–774 (2001)
DOI: 10.1051/0004-6361:20010547

Astronomy & Astrophysics

HI in Abell 3128

J. N Chengalur[1,4], R. Braun[2], and M. Wieringa[3]

[1] National Centre for Radio Astrophysics, Post Bag 3, Ganeshkind PO, Pune, Maharashtra 411 007, India
[2] Netherlands Foundation for Research in Astronomy, PO Box 2, 7990 AA Dwingeloo, The Netherlands
e-mail: rbraun@nfra.nl
[3] The Australia Telescope National Facility, PO Box 76, Epping, NSW 2121, Australia
e-mail: mark.wieringa@atnf.csiro.au
[4] Visiting Scientist, NFRA, PO Bos 2, 7990 AA Dwingeloo, The Netherlands

Received 25 October 2000 / Accepted 6 April 2001

Abstract. We discuss Australia Telescope Compact Array (ATCA) HI 21 cm data for the galaxy cluster A3128. Our observations are intentionally relatively shallow, and a blind search through our data cube yields (tentative) detections of only two galaxies, of which one is probably spurious. A3128 is part of the ESO Nearby Abell Cluster Survey (ENACS) (Katgert et al. 1996); redshifts are available for 193 galaxies in the A3128 region. For 148 of these galaxies the redshifts are such that the HI emission (if any) would lie within our data cube. We use the known redshifts of these galaxies to coadd their spectra and thus improve our sensitivity to HI emission. The technique is fairly successful – the coadded spectra allow detection of an average mass content of $\sim 9 \times 10^8\ M_\odot$, almost an order of magnitude lower than for direct detection (by which we mean a 5σ detection after smoothing to $90'' \times 90''$ and 300 $\mathrm{km\,s^{-1}}$ resolution) of individual objects. By dividing the total galaxy sample into subsamples we find that the gas content of late type galaxies that lie outside the X-ray emitting core of the cluster is substantially higher than that of those within the core. The fact that for disk galaxies the average gas content is higher for galaxies outside the X-ray emitting region as compared to those inside implies that these galaxies are not well mixed in the cluster potential. Even outside the X-ray emitting region the distribution of gas-rich galaxies in the cluster is not uniform, we find that gas-rich galaxies are concentrated in the east of the cluster. This is consistent with earlier analyses of the kinematics of the galaxies in A3128 which indicate the presence of subclustering. In summary we find that coadding spectra is a powerful tool for the study of HI in cluster galaxies, and suggest that this technique could be applied to substantially increase the redshift range over which such observations could be carried out.

Key words. galaxies: clusters: general – galaxies: clusters: individual: A3128 – galaxies: HI content – cosmology: observations – radio lines: galaxies

1. Introduction

There is growing evidence that environment plays an important role in galaxy evolution. In particular, for cluster galaxies, interaction with the inter-cluster medium (ICM) as well as gravitational interaction with other cluster members appears to play an important role. For example, numerical simulations suggest that the effect of multiple distant galaxy encounters ("galaxy harassment") suffered by a galaxy passing through a cluster is sufficient to change the morphology of a dwarf spiral into a dwarf spheroidal (Moore et al. 1996), as well as to sufficiently thicken the stellar disks of larger spiral galaxies to make them morphologically similar to S0s (Moore et al. 1999). Interaction with the ICM is expected to have an equally dramatic effect on the gas content of galaxies, with a combination of ram pressure and viscous stripping being sufficient to strip an $L_\star$ spiral of essentially all of its gas within 100 Myear (Quilis et al. 2000).

There is also considerable observational evidence for the effect of the cluster environment on galaxy evolution. Spiral galaxies in clusters are known to be deficient in HI as compared to field galaxies (Haynes et al. 1984). However, the molecular gas content (or at least the luminosity of the CO emission) appears to be the same for cluster and field galaxies (Kenney & Young 1989), suggesting that the gas removal mechanisms are most effective for the outer parts of the galaxy disk. Synthesis imaging of galaxies in the Virgo cluster has shown that galaxies near the cluster center have systematically smaller gas disks than those further out, and also that the gas disks are asymmetric and have sharp edges on the side closer to the cluster center (Cayatte et al. 1990). The efficient removal of gas also necessarily affects star formation – cluster galaxies are found to have suppressed star formation rates as compared to field galaxies (Balogh et al. 1998).

Send offprint requests to: J. N Chengalur,
e-mail: chengalur@ncra.tifr.res.in

Galaxy clusters, even at low redshifts, are still accreting material. Galaxy groups that are falling in to the cluster for the first time still have substantial gas content and can hence be easily identified from their HI emission (e.g. Coma, Bravo-Alfaro et al. 2000). Similarly, in the Virgo cluster, the HI deficient galaxies show considerable substructure (Solanes et al. 2001). Another aspect of the rapid recent evolution of clusters is that clusters at even modest redshift ($z < 0.5$) appear to have substantially different properties from those of local clusters. These clusters have a larger fraction of blue galaxies (Butcher & Oemler 1984) and also have a larger fraction of spirals and a smaller fraction of S0s as compared to local clusters (Dressler et al. 1997). The gas content of galaxies in moderate redshift clusters is, however, unknown, since the HI emission from a typical galaxy at these redshifts is too faint to detect with existing telescopes in reasonable integration times.

At the very lowest redshifts the HI content of clusters can be studied using single dish telescopes, however the poor angular resolution of these telescopes makes them unsuitable for studies of clusters even at redshifts of $\sim$0.1. At these redshifts however aperture synthesis observations are fairly efficient, since most of the cluster galaxies fall within a single primary beam.

We report here on observations of the $z = 0.06$ cluster A3128 made using the Australia Telescope Compact Array (ATCA). The observations were relatively shallow, but we coadd the spectra of the different galaxies to improve our detection threshold. The rest of this paper is organized as follows. The observations are discussed in Sect. 2, the search for HI emission from individual galaxies in Sect. 3.1, and the coadded spectra from different subsamples in Sect. 3.2. Section 4 contains a discussion of the main results from our analysis. Throughout the paper we use $H_0 = 75\,\mathrm{km\,s^{-1}/Mpc}$, $q_0 = 0.5$, $\Lambda = 0$ and the angular diameter distance or luminosity distance as appropriate. Also, "heliocentric velocities" is used throughout this paper to mean the quantity cz where z is the heliocentric redshift.

2. Observations and data reduction

The observations were conducted at the ATCA from 17 to 20 November 1996. All observations were conducted in the 750A array configuration. In this configuration 5 antennas are stationed such that they give baselines between 77 m and 735 m, the 6th antenna is much more distant and its baselines with the inner 5 antennas vary from 3015 m to 3750 m. Only the data from the 5 inner ATCA antennas were used in all the processing described below. Since A3128 is somewhat extended compared to the ATCA primary beam ($\sim 33'$) the observations were conducted in a compact mosaic of four pointing centers. The center frequency was 1339.0 MHz ($z \sim 0.06$) for all the observations. The bandwidth was 32 MHz ($\sim$7600 $\mathrm{km\,s^{-1}}$) and there were a total of 256 spectral channels, giving a channel spacing of $\sim$28 $\mathrm{km\,s^{-1}}$.

Table 1. Observation log.

RA(J2000)	DEC(J2000)	ν (MHz)	τ (hr)
3:31:00.01	−52:45:21.3	1339.0	9.8
3:31:00.01	−52:32:37.7	1339.0	9.6
3:29:36.20	−52:32:37.7	1339.0	9.6
3:29:36.20	−52:45:21.3	1339.0	9.6

The observations were spread over 4 twelve hour sessions, and each pointing center was observed once every session. The total integration time per pointing center is given in Table 1. The standard AT calibrator 1934-638 was observed once every observing session to determine the absolute flux scale. Phase and bandpass calibration were done using the source 0407-658, which was observed once every 30 m.

The data were analyzed using standard tasks from the MIRIAD package. Continuum was subtracted using a second order polynomial fit to the uv data; channels 30 to 239 were used to make the fit. The data from all pointing centers were used (after primary beam correction) to make a single naturally weighted mosaiced cube with a pixel size of $15''$ and a resolution of $81'' \times 53''$ which corresponds to about 85×56 kpc. The edge channels were discarded while making the cube, only channels 30 to 239 (which corresponds to a velocity coverage of $\sim$6200 $\mathrm{km\,s^{-1}}$) were used. The rms noise per channel is $\sim$1.3 mJy with slight variation over the region used for analysis.

3. Analysis

3.1. HI from individual galaxies

Our observations are relatively shallow, the 5σ mass limit corresponding to a Gaussian signal with FWHM 300 $\mathrm{km\,s^{-1}}$ is $M_{\mathrm{HI}} \sim 8 \times 10^9\ M_\odot$, comparable to the $M^*_{\mathrm{HI}} \sim 1 \times 10^{10}\ M_\odot$ of local field galaxies (e.g. Zwaan et al. 1997, corrected for our adopted H_0 of 75 $\mathrm{km\,s^{-1}/Mpc}$). Since our spatial coverage is also limited to only $\sim$1.5 Abell radii, and galaxies out to $\sim$2 Abell radii are substantially HI deficient (Solanes et al. 2001) it is not very surprising that visual inspection of the data cube yielded no obvious detection.

A statistically robust blind search was then made over the entire data cube. Assuming that the distributions of intensities in the cube is Gaussian, the probability of finding an intensity (purely by chance) in excess of a given threshold can be computed. The threshold was set such that the expected number of independent pixels above the threshold in the entire data cube was 0.5. The search was done (using the AIPS task SAD) at the original spatial resolution, as well as with the spatial resolution degraded (via smoothing in the image plane) to $90'' \times 90''$, and for velocity resolutions of 28, 56, 112, 224, and 448 $\mathrm{km\,s^{-1}}$. Only two "detections" were found in this blind search; the corresponding spectra are shown in Fig. 1. Table 2 lists the parameters derived from these spectra, along with the data for the nearest cataloged galaxies. Note that neither

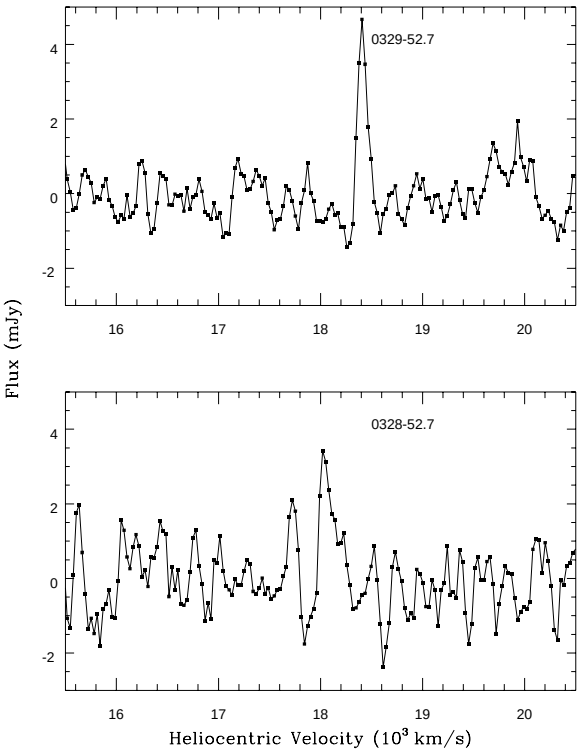

Fig. 1. Spectra of the two locations in the HI cube with emission greater than the threshold value. The threshold value was chosen such that the expected number of spurious detections in the entire cube is ∼0.5. The search for emission was "blind", i.e. over the entire cube without regard to the location of the cataloged galaxies.

of these two galaxies have a measured optical redshift, so they do not enter into the sample of galaxies whose spectra we coadd (see Sect. 3.2).

The columns in Table 2 are as follows. Column 1: Name of the nearest galaxy (IAU Format), Col. 2: Right Ascension of the nearest galaxy (J2000), Col. 3: Declination of the nearest galaxy (J2000), Col. 4: The angular separation (α, δ), in arc-seconds between the nearest cataloged optical galaxy and the HI signal, Col. 5: Heliocentric velocity of the HI signal, Col. 6: Peak Flux (mJy) of the HI signal, Col. 7: Integrated Flux (Jy km s^{-1}) of the HI signal, and Col. 8: Morphological Type (from Dressler 1980).

Note that our search criteria are generous in that we have ignored the uncertainties that would arise from the small deviations of the noise statistics from a Gaussian distribution. One should hence regard these detections as tentative. For 0328-52.7 the HI emission peak is fairly distant from the optical galaxy, the detection may be spurious. The HI detection of 0329-52.7 is, however, probably reliable. Figure 2 shows an overlay of the HI data and the optical data for this galaxy. This rigorous search for signals associated with known galaxies is also useful in interpreting the results of the next stage of our analysis, namely coadding of the spectra of individual galaxies.

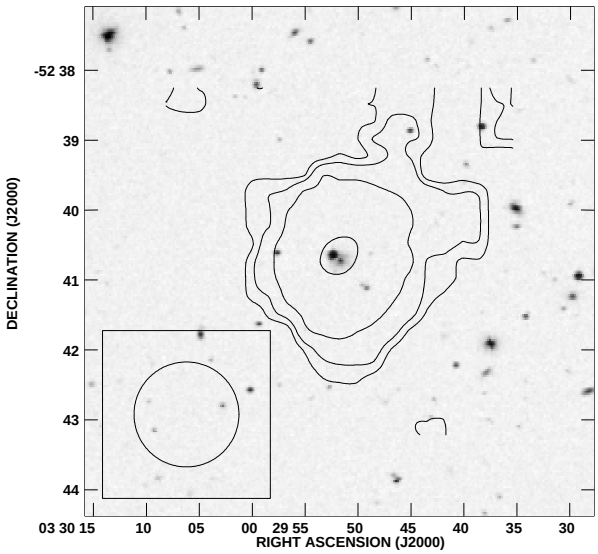

Fig. 2. The HI 21 cm contours overlayed over the optical (POSS II) image of 0329-52.7. The HI beam ($90'' \times 90''$) is shown in the bottom left corner. The contour levels are 0.5, 0.1, 0.2, and 0.4 Jy/Bm km s^{-1}.

3.2. Average HI content

As discussed in the previous subsection, because our observations are relatively shallow, we have what are, at best, tentative detections of two galaxies. A3128 is one of the clusters in the ESO Nearby Abell Cluster Survey (ENACS), and from multi-fiber spectroscopy, the redshifts of 193 galaxies in and around A3128 are available (Katgert et al. 1996; Katgert et al. 1998). These redshifts are typically accurate to ∼50 km s^{-1} or better. It should hence be possible to considerably improve our sensitivity by coadding the spectra of all of these galaxies. Of course, by doing so one is restricted to measuring the average HI content of the galaxies in the cluster, information on individual galaxies is lost. However, as we shall show, a judicious choice of subsamples makes coaddition a fairly powerful analysis technique.

We start by looking at the average signal from known ENACS galaxies within the cluster. The spectra at the location of each galaxy whose redshift is known were extracted from the $90'' \times 90''$ resolution cube, shifted along the velocity axis so that any HI signal present would appear in the same channel for all spectra, and then averaged together. In the averaging process each spectrum is weighted according to its rms (recall that the noise level varies slightly across our cube, because of the loss in sensitivity at the edges of the mosaic). The averaged spectrum (all the averaged spectra shown in this section have been smoothed to a velocity resolution of ∼140 km s^{-1}) is shown in Fig. 4a. The velocity to which all the spectra have been shifted is shown by a short vertical line. Figure 4b shows another average of these same spectra, the difference being that the velocity shifts are randomized, i.e. the shift for one galaxy is randomly applied to some other galaxy. By using the same set of shifts for both

Table 2.

Name	RA J2000	Dec J2000	Δ(Ra,Dec) arc-sec	$V_{\rm HI}$ km s^{-1}	$S_{\rm peak}$ mJy	$S_{\rm int}$ Jy km s^{-1}	$M_{\rm HI}$ 10^9 $M_\odot$	Type
0328-52.7	03:28:04.1	−52:44:41.3	41 9	18021 ± 30	3.9 ± 1.3	0.45 ± 0.1	6 ± 1.3	...
0329-52.7	03:29:51.5	−52:40:44.7	4 16	18407 ± 30	5.5 ± 1.3	0.45 ± 0.1	6 ± 1.3	S

the average spectra we ensure that the statistics of the shifts applied to the coherently added as well as the randomly added spectra are the same. As can be seen there is a weak signal (peak $S/N = 3.5$) present at the correct velocity in the coherently averaged spectrum.

Galaxies near the center of the cluster are expected to have lower average HI content, both because of the morphology-density relation (i.e. because earlier morphological types which have inherently little HI are dominant in the high density core) and also because the HI deficiency of late type galaxies increases towards the cluster center (Cayatte et al. 1990; Solanes et al. 2001). We have consequently constructed a subsample consisting of only those galaxies which lie (in projection) outside the X-ray contours shown in Fig. 3. The coadded signal from this subsample is shown in Fig. 4c, while the randomized average spectrum (i.e. the one with the same galaxies, but with the velocities scrambled before averaging) is shown in Fig. 4d. Both the strength and significance (peak $S/N = 4.0$) of the signal seen in Fig. 4a are slightly increased by excluding the galaxies within the X-ray contours.

In principle it might have been possible that the signal seen after coadding the spectra came from just one or two bright galaxies. In this particular case it is unlikely because, as we discussed in Sect. 3.1, we have no clear detection of any individual galaxy in the sample. As a further test every individual spectrum was clipped at 2.5σ (where σ is the rms in the original individual spectra), the clipped and non clipped coadded spectra are essentially identical.

Having been successful in detecting the averaged HI signal from all galaxies in the cluster, one could try and determine the averaged HI signal from appropriately chosen subsamples. Thirty galaxies in the A3128 sample show optical emission lines. Biviano et al. (1997) find that the emission-line galaxies in the ENACS sample are generally spiral galaxies, i.e. that emission-line galaxies are spirals, but that not all spirals are emission-line galaxies. The coadded signal for all the emission-line galaxies in A3128 is shown in Fig. 5a, and for all emission-line galaxies outside the X-ray contours in Fig. 5c. As before, the comparison randomized average spectra are shown in Figs. 5b and 5d respectively. The peak signal-to-noise ratio in both cases is very low (2.6 and 2.7 respectively) since relatively few galaxies were available. In any case, it is possible to state that the emission-line galaxies do not provide a dominant contribution to the average gas mass.

Morphological types (from Dressler 1980) are also available for 130 galaxies in A3128 for which redshift information is also available from the ENACS survey. Of these

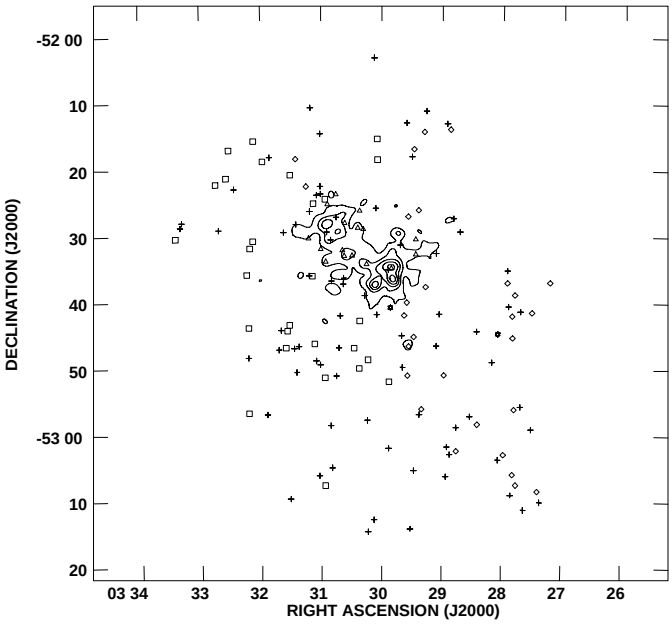

Fig. 3. Position of galaxies in A3128 that have measured redshifts and lie within our HI data cube. The X-ray emission (from a ROSAT HRI broadband image) is shown as contours. The two galaxies whose HI emission has been tentatively detected (see Sect. 3.1) are shown as stars. Neither of these two galaxies has an optically measured redshift. Late type galaxies are shown as hollow squares, hollow diamonds and hollow triangles. The hollow squares are "gas rich" on the average, while the hollow diamonds are "gas poor" on the average. See Sect. 3.3 for the definition of "gas rich" and "gas poor". Galaxies which are regarded as lying within the X-ray emitting region are shown as hollow triangles. Crosses are either early type galaxies, or galaxies whose morphological type is unknown.

130 galaxies, 108 lie within our data cube. The coadded signal from all the galaxies of type S0 and later (where we have deliberately regarded S0s as "late-types" to account for uncertainties in the morphological typing) is shown in Fig. 6a. The coadded signal for the subset of these galaxies that lie outside the X-ray contours is shown in Fig. 6c. The comparison randomized average spectra are shown in Figs. 6b and 6d respectively. In this case a large enhancement in both signal strength and peak signal-to-noise ratio (changing from 2.8 to 4.0) is seen on constraining the sample to avoid the cluster core.

If one restricts the morphological types included in the sample to Sa's and later (including types classified only as "S") no significant signal is found. There are a total of 28 such galaxies (24 outside the X-ray contours).

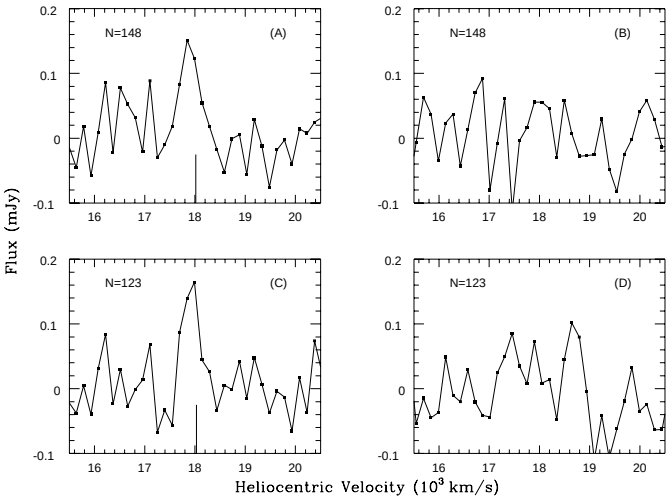

Fig. 4. Average and control HI spectra using all ENACS galaxies in A3128 with measured redshift. **a)** Average spectrum over all 148 galaxies. **b)** Control spectrum for **a)** with randomized velocity shifts. **c)** Average spectrum over the 123 galaxies outside the cluster core. **d)** Control spectrum for **c)** with randomized velocity shifts. All spectra have been smoothed to a velocity resolution of $\sim$140 km s^{-1}.

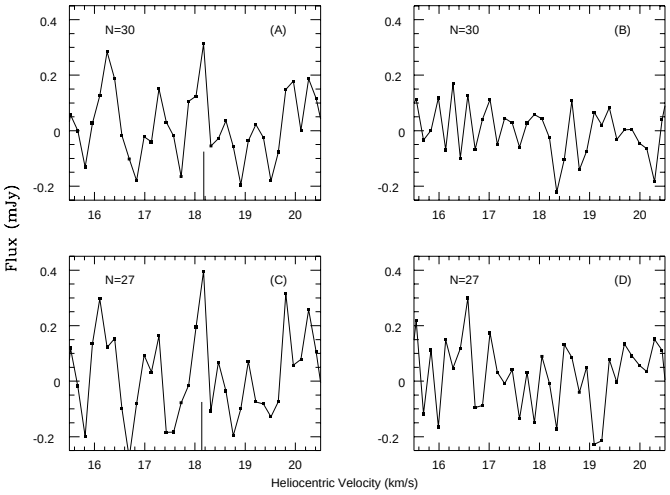

Fig. 5. Average and control HI spectra of emission-line ENACS galaxies in A3128 with measured redshift. **a)** Average spectrum over all 30 emission-line galaxies. **b)** Control spectrum for **a)** with randomized velocity shifts. **c)** Average spectrum over the 27 emission-line galaxies outside the cluster core. **d)** Control spectrum for **c)** with randomized velocity shifts. All spectra have been smoothed to a velocity resolution of $\sim$140 km s^{-1}.

3.3. Substructure

As we have already seen in Sect. 3.2, the galaxies that lie outside the X-ray contours are more gas-rich on average. Also, the strongest emission signal is found for galaxies with late morphological types and which lie outside the X-ray contours, in line with what would be expected from theoretical models and existing HI observations of clusters.

We also tried to examine the distribution of gas-rich galaxies to check if the average gas content (even for

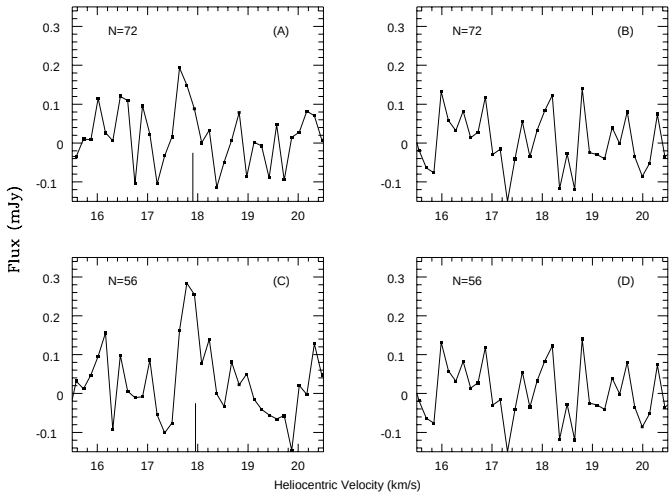

Fig. 6. Average and control HI spectra of ENACS galaxies in A3128 with morphological type S0 or later and measured redshift. **a)** Average spectrum over all 72 late-type galaxies. **b)** Control spectrum for **a)** with randomized velocity shifts. **c)** Average spectrum over the 56 late-type galaxies outside the cluster core. **d)** Control spectrum for **c)** with randomized velocity shifts. All spectra have been smoothed to a velocity resolution of $\sim$140 km s^{-1}.

galaxies outside the X-ray contours) varies with position or not. The procedure we used is as follows. For each of the 56 late type galaxies outside the X-ray contours we determined the nearest 20 neighbors (including the target galaxy itself; by "nearest" we mean the 20 galaxies with the smallest angular distance from the target galaxy). The spectra of this group were then coadded. For all channels within $\pm$10 channels (i.e. within $\sim\pm$280 km s^{-1}) of the expected HI signal the ratio of the flux in the channel to the expected rms noise in the coadded spectrum (i.e. as computed from the rms of the individual spectra and the number of spectra which contribute to that channel) was computed. This maximum "signal to noise ratio" is recorded for each galaxy. Target galaxies for which this number is greater than the median for the entire sample (i.e. "gas-rich") are shown in Fig. 3 as hollow squares, and galaxies for which the number is less than the median (i.e. "gas-poor") are shown as hollow diamonds. Galaxies which are regarded as lying within the X-ray emitting region (and omitted from this analysis) are shown as hollow triangles. As can be seen, the distribution is far from random, the "gas-rich" galaxies are concentrated on the east part of the cluster. The coadded spectrum with the highest signal to noise ratio is shown in Fig. 7. The HI mass corresponding to this spectrum is $\sim 2.6 \times 10^9\ M_\odot$, and the $< M_{\rm HI} > / < L_R >$ is $\sim$0.1. If one uses the entire sample, instead of only the late type galaxies, one gets essentially the same result, namely that the galaxies in the east half of the cluster are more gas-rich on average than those in the west.

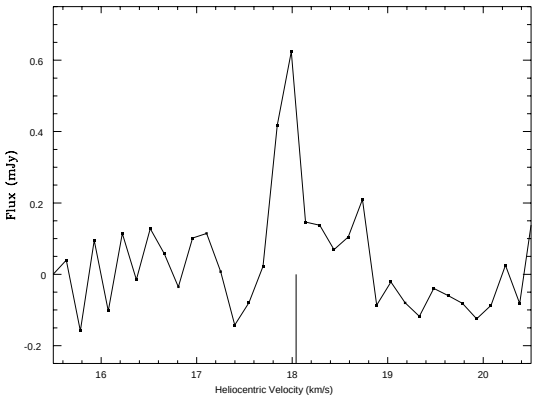

Fig. 7. The coadded spectrum smoothed to 140 $\mathrm{km\,s^{-1}}$ velocity resolution for the group of 20 galaxies with the most significant emission signal. Groups are defined purely on the basis of proximity in projected separation and independent of HI content of the individual galaxies. See Sect. 3.3 for details.

4. Discussion

Abell 3128 is a richness class 3, Bautz-Morgan Type I-II cluster (Abell et al. 1989) with an X-ray luminosity in the 0.5−2 keV band of 1.62×10^{44} ergs/s (de Grandi et al. 1999). Redshifts of 193 galaxies in this field are available from the ENACS survey (Katgert et al. 1996). The HI cube is centered at $\alpha_{2000} =$ 03h30m20s, $\delta_{2000} = -52$d39m15s and is $<85'$ on a side, which corresponds to a diameter of <3 Abell radii. 148 of the 193 galaxies for which radial velocities are available lie within our HI cube.

The derived quantities corresponding to the spectra in Figs. 4 to 6 are summarized in Table 3. The columns in the table are as follows: Col. 1: Sample name, i.e. (a) all the galaxies in the sample, (b) all galaxies outside the X-ray contours, (c) all galaxies with emission lines, (d) all galaxies with emission lines and outside the X-ray contours, (e) all galaxies typed S0 and later, and (f) all galaxies typed S0 and later which lie outside the X-ray contours, Col. 2: Number of galaxies in the sample, Col. 3: The HI mass that the spectrum corresponds to. The mass is computed from the equation

$$M_{\rm HI} = 2.35 \times 10^5 D^2 \int S(v) \mathrm{d}v \qquad (1)$$

where $M_{\rm HI}$ is the HI mass in units of solar masses, D is the luminosity distance in Mpc (∼240 Mpc in this case), the flux S is in Jy and the velocity v in $\mathrm{km\,s^{-1}}$. The error in the computed HI mass scales as $\sqrt{N_{\rm chan}}\sigma$, where $N_{\rm chan}$ is the number of channels over which the signal is spread and σ is the rms noise in the coadded spectrum. For this data set at least, the velocity width of the signal in general increases as the sample size increases. The error in the HI mass hence does not scale as $\sqrt{N_{\rm gal}}$ as might have been expected a priori, Col. 4: The velocity width of the signal. This is the FWHM of the best fit Gaussian, Col. 5: The average R band luminosity of the galaxies in the sample, and Col. 6: The ratio of the HI mass to the average luminosity.

Table 3. Averaged HI content.

Sample	N	$< M_{\rm HI} >$ $10^8\ M_\odot$	ΔV $(\mathrm{km\,s^{-1}})$	$< L_{\rm R} >$ $10^{10}\ L_\odot$	$\frac{<M_{\rm HI}>}{<L_{\rm R}>}$ $M_\odot/L_\odot$
All	148	8.5 ± 2.0	420 ± 47	2.3	0.04
All-out	123	8.6 ± 2.0	370 ± 47	2.2	0.04
Em	30	8.7 ± 2.6	184 ± 55	1.6	0.05
Em-out	27	10.4 ± 2.6	179 ± 55	1.7	0.06
Late	72	8.6 ± 2.2	330 ± 45	2.5	0.04
Late-out	56	16.7 ± 2.6	394 ± 45	2.4	0.07

We note that our sample is not unbiased, since in the ENACS survey redshifts are generally available only for the brighter galaxies. Further, the ENACS sample is not a simple magnitude limited sample because the ease with which the redshift can be measured depends on the average central surface brightness and there is no simple relation between the average central surface brightness and the total magnitude. The ENACS galaxy sample itself (i.e. independent of whether redshifts were measurable or not) is complete to $r_{25} \sim 16.5$, which, for a distance of 240 Mpc, corresponds to an absolute magnitude of ∼−20.4. We are hence insensitive to galaxies fainter than $\sim L^*$. From surveys of field spirals we know that the gas content (by mass) increases with luminosity and that large spirals are the dominant contributors to the total gas mass in galaxies (Rao & Briggs 1993). In cluster environments Valluri & Jog (1991) had found a tendency for HI deficiency to increase with increasing optical size, however Solanes et al. (2000), using a much larger sample size, found no such trend. One would hence expect that even in cluster environments, the bulk of the gas content would be in large spiral galaxies.

As was already evident from Figs. 4 to 6, the average gas content of galaxies outside the X-ray contours is larger than that of those inside (as expected both from the morphology-density relationship and also from processes in which interaction with the hot ICM strips the neutral gas from galaxies). In fact, within the measurement accuracy, our data are consistent with all the detected gas coming from late type galaxies outside the X-ray contours. (i.e. the total HI mass in all the cluster galaxies is equal, within 2σ, to the total HI mass in late type galaxies outside the X-ray contours.) However the fact that even for the "late" subsample the average HI content of the galaxies outside the X-ray contours is larger than that of those inside the contours suggests that some kind of gas stripping mechanism due to interaction with the ICM must be in operation. It is interesting that the galaxies "know" where the X-ray contours are. If the cluster was well mixed, then the probability that a given galaxy has at some time passed through the cluster core would be independent of its current position, contrary to what is observed.

Solanes et al. (1999) have investigated the existence of substructure in the ENACS sample using

diagnostics that are sensitive to the presence of substructure, but which do not identify the individual substructures themselves. While all the diagnostics suggested the presence of substructure in A3128, the Δ test (Dressler & Schectman 1988) in particular gives a probability of $<10^{-3}$ that there is no substructure in A3128. Similarly, Biviano et al. (1997) use the Δ test to find a probability $<10^{-3}$ that there is no substructure in both the entire A3128 galaxy sample, as well as the subsample consisting only of non-emission-line galaxies. van Gorkom (1996) showed that HI content is a good indicator for substructure, HI rich galaxies are largely confined to groups that are falling into the cluster for the first time. Our test for substructure, although necessarily of poorer spatial resolution, is also indicative of the presence of substructure, the gas-rich galaxies are confined to the east of the cluster. The group of 20 galaxies whose coadded spectrum is shown in Fig. 7 have on the average $\sim$2.5 times more HI than the remaining late type galaxies outside the X-ray contours.

Biviano et al. (1997) found that emission-line galaxies are a subset of spiral galaxies. De Theije & Katgert (1999) suggest that the emission-line galaxies are those spirals which have either never passed through the core of the cluster or are passing through the core of the cluster for the first time. Emission-line galaxies would then be expected to have a larger HI content than the average spiral galaxy, however from Table 2 we find that the average gas content of the emission-line galaxies and the late type galaxies is comparable (when one considers the entire subsample). For galaxies which lie outside the X-ray contours however, late type galaxies are, on the average, more gas-rich than emission-line galaxies.

It is worth noting that the average HI mass that we are sensitive to is $\sim 9 \times 10^8\ M_\odot$, i.e. almost a factor of 10 less than the 5σ limit computed in Sect. 3.1 for an individual detection. This makes this technique highly suitable for extending the redshift range of HI observations of clusters. In particular, with the WSRT, VLA or GMRT sensitivities, it should be possible to measure the average HI content of clusters out to redshift of $\sim$0.5 in reasonable observing times. This is an extremely interesting redshift range since from ground based as well as HST observations it is now established that there is considerable evolution of cluster galaxies between redshifts of 0 and 0.5. Indeed after submission of this paper, we learnt that a similar technique had been independently used by Zwaan (2000) to study the $z = 0.2$ cluster A2218.

At cosmological redshifts, the number density of Lyman-break galaxies with redshifts between $3.0 < z < 3.5$ is $\sim$0.4 per square arcmin (Steidel et al. 1996). This means that about 3000 of these galaxies are contained within a single GMRT primary beam (and a single correlator setting). The excellent GMRT sensitivity at $z = 3.3$ (Swarup et al. 1991) means that coadding the spectra should allow detection of an average HI mass of $\sim 10^{10}\ M_\odot$ in an integration time of $\sim$100 hr.

Acknowledgements. This paper is based on observations with the Australia Telescope Compact Array, which is funded by the Commonwealth of Australia for operation as a National Facility managed by CSIRO. This research has made use of data obtained through the High Energy Astrophysics Science Archive Research Center Online Service, provided by the NASA/Goddard Space Flight Center. This work was partly funded by a bezoekersbeurs from NWO to JNC. We are grateful to the referee (J. H. van Gorkom) for a very careful reading of the paper and numerous valuable comments, to R. Fanti for assistance with the data analysis, and to P. Katgert for having supplied the ENACS redshifts in advance of publication. Nissim Kanekar's numerous suggestions have greatly improved the readability of this paper.

References

Abell, G. O., Corwin, H. G. Jr., & Olowin, R. P. 1989, ApJS, 70, 1
Balogh, M. L., Schade, D., Morris, S. L., et al. 1998, ApJ, 504, L75
Biviano, A., Katgert, P., Mazure, A., et al. 1997, A&A, 321, 84
Bravo-Alfaro, H., Cayatte, V., van Gorkom, J. H., & Balkowski, C. 2000, AJ, 119, 580
Butcher, H., & Oemler, A. Jr. 1984, ApJ, 285, 426
Cayatte, V., van Gorkom, J. H., Balkowski, C., & Kotanyi, C. 1990, AJ, 100, 604
Cayatte, V., Kotanyi, C., Balkowski, C., & van Gorkom, J. H. 1994, AJ, 107, 1003
de Grandi, S., Böhringer, H., Guzzo, L., et al. 1999, ApJ, 514, 148
de Thije, P. A. M., & Katgert, P. 1999, A&A, 341, 371
Dressler, A. 1980, ApJS, 42, 565
Dressler, A., & Schectman, S. A. 1988, AJ, 95, 985
Dressler, A., Oemler, A. Jr., Couch, W. J., et al. 1997, ApJ, 490, 577
Moore, B., Katz, N., Lake, G., Dressler, A., & Oemler, A. Jr. 1996, Nature, 379, 613
Moore, B., Lake, G., Quinn, T., & Stadel, J. 1999, MNRAS, 304, 465
Haynes, M. P., Giovanelli, R., & Chincarini, G. L. 1984, ARA&A, 22, 445
Katgert, P., Mazure, A., Perea, J., et al. 1996, A&A, 310, 8
Katgert, P., Mazure, A., den Hartog, R., et al. 1998, A&AS, 129, 399
Kenney, J. D. P., & Young, J. S. 1989, ApJ, 344, 171
Quilis, V., Moore, B., & Bower, R. 2000, Science, 288, 1617
Rao, S., & Briggs, F. H. 1993, ApJ, 419, 515
Solanes, J. M., Salvador-Solé, E., & González-Casado, G. 1999, A&A, 343, 733
Solanes, J. M., Manrique, A., García-Gómez, C., et al. 2001, ApJ, 548, 97
Steidel, C. C., Giavalisco, M., Pettini, M., Dickinson, M., & Adelberger, K. L. 1996, ApJL, 462, L17
Swarup, G., Ananthakrishnan, S., Kapahi, V. K., et al. 1991, Current Science, 60, 95
Valluri, M., & Jog, C. J. 1991, ApJ, 374, 103
van Gorkom, J. H. 1996, PASP Conf. Ser., 106, 293
Zwaan, M. A., Briggs, F. H., Sprayberry, D., & Sorar, E. 1997, ApJ, 490, 173
Zwaan, M. A. 2000, Ph.D. Thesis, Groningen Univ.